



NO reduction by CO over gold catalysts based on ceria supports, prepared by mechanochemical activation, modified by Me³⁺ (Me = Al or lanthanides): Effect of water in the feed gas

L. Ilieva^{a,*}, G. Pantaleo^b, R. Nedyalkova^a, J.W. Sobczak^c, W. Lisowski^c, M. Kantcheva^d, A.M. Venezia^b, D. Andreeva^a

^a Institute of Catalysis, Bulgarian Academy of Sciences, Acad. G. Bonchev str., bl.11, Sofia 1113, Bulgaria

^b Istituto per lo Studio Di Materiali Nanostrutturati, CNR, Palermo I-90146, Italy

^c Institute of Physical Chemistry, PAS, Kasprzaka 44/52, 01-224 Warszawa, Poland

^d Department of Chemistry, Bilkent University, 06800 Bilkent, Ankara, Turkey

ARTICLE INFO

Article history:

Received 28 November 2008

Received in revised form 13 March 2009

Accepted 16 March 2009

Available online 25 March 2009

Keywords:

Gold

Ceria modified by Al, La, Sm, Gd or Yb

Mechanochemical activation

NO reduction by CO

Effect of water

ABSTRACT

The reduction of NO by CO was studied over gold catalysts supported on ceria modified by Me³⁺ ions (Me = Al, La, Sm, Gd and Yb). The ceria supports were prepared by mechanochemical activation. The samples were characterized using XRD, TPR, XPS and Raman spectroscopy. According to the XPS data the concentration of the oxidized gold species was higher than that of metallic gold in the fresh samples modified by lanthanides. On the fresh samples modified by Al only a small part of metallic gold existed in oxidized state. After the catalytic test, only metallic gold was found on the lanthanide-containing catalysts while on the Al-modified catalyst a small amount of oxidized Au species in addition to metallic Au was detected. No substantial differences in the average particle sizes of gold, the lattice parameters and the average size of ceria particles were observed. The nature of the modifier and the applied method of ceria supports preparation and gold deposition determined most likely the differences observed in the Raman and TPR data, as well as the catalytic activity results. The catalytic tests were performed under two different conditions: (i) in the presence of H₂ in the gas feed and (ii) adding also water to the gas feed. The lowest activity was observed over the Al-containing catalyst under dry feed, which correlates with the TPR results. The addition of water to the feed led to a significant improvement of the NO and CO conversions over all of the samples studied. At 200 °C, Yb-containing gold catalyst exhibited the highest NO and CO conversions. Very promising results for the selectivity toward N₂ were achieved using the lanthanides as dopants. In contrast to the gold supported on Al-doped ceria, no NH₃ formation was observed within the whole temperature interval up to 400 °C over gold catalysts supported on ceria modified by La, Sm, Gd or Yb.

© 2009 Elsevier B.V. All rights reserved.

1. Introduction

The catalytic reduction of NO_x (DeNO_x) has been extensively investigated in view of lowering the harmful vehicles' emissions. A large amount of efforts has been expended studying platinum, palladium and rhodium containing catalysts. In the last decades one of the most surprising and significant results in the field of catalysis was the finding that nano-structured gold catalysts supported on different metal oxides are highly active at relatively low temperatures in several reactions of technological importance [1–3]. Also, it has been established that supported nanosized gold behaves as a

catalytically active metal in the NO_x reduction by H₂, CO or hydrocarbons [4–10]. The low temperature activities of such gold based catalysts make them very promising for DeNO_x of the exhaust gases emitted at the start-up of the vehicle's engine ("cold start" phase). Our results on the reduction of NO by CO have shown a high activity and 100% selectivity toward N₂ at about 200 °C in the presence of gold catalysts, supported on mixed ceria–alumina prepared by co-precipitation (CP) [11,12] or by mechanochemical activation (MA) [13]. It has been established that if hydrogen is present in the feed gas, the reduction of NO by CO is strongly enhanced but hydrogen is not an effective reducing agent in the low temperature (LT) range, which is of interest concerning gold based catalysts. The addition of water to the feed significantly improves the NO reduction activity by CO due to the production of hydrogen by WGS, thus keeping 100% selectivity to N₂ at about 200 °C. Alumina in

* Corresponding author. Fax: +359 2 971 2967.

E-mail address: luilieva@ic.bas.bg (L. Ilieva).

the mixed supports acts as a structural promoter, which prevents the agglomeration of both gold and ceria particles during the catalytic operation. Moreover, the presence of alumina leads to the modification of ceria. We found that the preparation method and amount of doped alumina affect ceria support. It has been established that keeping the same alumina content, the amount of oxygen vacancies in ceria–alumina carriers synthesized by the CP method was higher than that of the samples prepared using the MA procedure. Higher conversions of both NO and CO were obtained in the case of gold catalysts supported on ceria–alumina synthesized by the CP method. Upon doping ceria with Me^{3+} ions, the crystal lattice must compensate for the excess negative charge in principle by three mechanisms: vacancy compensation, cerium interstitial compensation and dopant interstitial compensation. For small cations with radius $<0.8 \text{ \AA}$ the vacancy compensation is accompanied by some compensation via dopant interstitial mechanism, while in the case of Me^{3+} dopants with radius $>0.8 \text{ \AA}$, the vacancy compensation is the preferable route [14]. Having in mind the radii of lanthanide ions used as dopants, the preferential route of vacancy compensation should be expected. Recently we started investigations of gold catalysts supported on ceria modified by lanthanide oxides. The preliminary Raman spectroscopy data indicate that the structure of ceria support of such gold catalysts depends on the preparation procedure; much more defective ceria structure seems to be formed after the MA than CP method. This trend is opposite to the tendency reported for gold catalysts supported on ceria doped by alumina [13].

The already established correlation between the catalytic activity in the NO reduction by CO and the amount of oxygen vacancies in the structure of ceria motivated us to focus the present investigation on nanosized gold deposited on ceria, modified by lanthanides (La, Sm, Gd, and Yb) using mechanochemical method for supports' preparation. The effect of the Me^{3+} modifier – aluminum or lanthanide metal cation – on the properties of the catalysts and their activity and selectivity in the NO reduction by CO was compared. Since the exhaust gases usually contain water vapour at a concentration up to 10 vol.% a special attention was paid on the selectivity toward N_2 in the presence of water in the feed gas.

2. Experimental

2.1. Catalysts preparation

Ceria supports modified by 10 wt.% Me^{3+} (Me = Al, La, Sm, Gd and Yb) were synthesized by mechanochemical method using a freshly prepared vacuum dried cerium hydroxide. The cerium hydroxide was obtained by precipitation of cerium nitrate with a solution of K_2CO_3 . A mixture of cerium hydroxide and the corresponding Me_2O_3 was subjected to mechanochemical activation by milling for 30 min in a mortar and calcination at $400 \text{ }^\circ\text{C}$ for 2 h. Then, before deposition of gold hydroxide, the modified ceria supports were additionally dispersed in water using an UV disintegrator "Ultrasonic UD-20 automatic" under vigorous stirring to improve homogeneity. The supports are denoted as CeAl, CeLa, CeSm, CeGd and CeYb, respectively. Gold was loaded by deposition–precipitation method. The deposition of gold on the support suspended in water, was performed via interaction of $\text{HAuCl}_4 \cdot 3\text{H}_2\text{O}$ and K_2CO_3 at constant pH 7.0 and temperature of $60 \text{ }^\circ\text{C}$. After aging for 1 h, the precipitate was carefully washed, dried in vacuum at $80 \text{ }^\circ\text{C}$ and calcined in air at $400 \text{ }^\circ\text{C}$ for 2 h. The gold loading was 2 wt.% for the catalysts supported on ceria, doped by lanthanides and 2.9 wt.%—for the Al-containing sample. The syntheses were carried out in a "Contalab" laboratory reactor enabling complete control of the reaction parameters (pH, temperature, stirrer speed, reactant feed flow, etc.) and high reproducibility. The used reagents were "analytical grade" of

purity. The gold catalysts are denoted as AuCeAl, AuCeLa, AuCeSm, AuCeGd and AuCeYb, respectively.

2.2. Catalyst characterization

The BET surface area of the samples was determined on a Micromeritics 'Flow Sorb II-2300' device with 30% N_2 , 70% He mixture at atmospheric pressure and N_2 boiling temperature.

The X-ray diffraction measurements were performed with an automatic powder diffractometer DRON (Bragg-Brentano arrangement), using $\text{Cu K}\alpha$ radiation and a scintillation counter. The diffraction patterns were recorded in a step-scan mode with a step of 0.02° (2θ), counting time 1 s, in the angular interval $20\text{--}90^\circ$ (2θ). The Powder Cell program [16] was used for diffraction data processing. The program gives the possibility of approximation of XRD spectra based on the corresponding theoretical structures. The instrumental broadening was taken into consideration. XRD profiles were approximated by Lorentz functions.

The Raman spectra were recorded using a SPEX 1403 double spectrometer with a photomultiplier, working in the photon counting mode. The 488 nm line of an Ar^+ ion laser was used for excitation. The laser power on the samples was 60 mW. The samples were prevented from overheating during the measurements by increasing the size of the focused laser spot. The optimal conditions were chosen, checking the intensity, the position and the width of the 464 cm^{-1} Raman line of CeO_2 . The spectral slit width was 4 cm^{-1} .

The TPR measurements were carried out by means of an apparatus described elsewhere [17]. A cooling trap ($-40 \text{ }^\circ\text{C}$) for removing water formed during the reduction was mounted in the gas line prior to the thermal conductivity detector. A hydrogen–argon mixture (10% H_2), dried over a molecular sieve 5A ($-40 \text{ }^\circ\text{C}$), was used to reduce the samples at a flow rate of 24 ml min^{-1} . The temperature was linearly raised at a rate of $15^\circ \text{ min}^{-1}$. The sample mass used was 0.05 g. It was selected by the criterion proposed by Monti and Baiker [18]. In addition TPR experiments after reoxidation were performed. The reoxidation was carried out with purified air at the temperature, immediately after the end of the first TPR peak ($200 \text{ }^\circ\text{C}$) of the fresh sample. The H_2 –Ar flow was switched to an air flow for 15 min and after cooling to room temperature in purified helium, a new TPR measurement was started. The hydrogen consumption during the reduction processes was calculated using preliminary calibration of the thermal conductivity detector, performed by reducing different amounts of NiO to Ni^0 (NiO —"analytical grade" of purity, calcined for 2 h at $800 \text{ }^\circ\text{C}$ to avoid the presence of Ni^{3+} ions).

The X-ray photoelectron spectroscopy data were recorded on a VG Scientific ESCALAB-210 spectrometer using Al $\text{K}\alpha$ radiation (1486.6 eV) from an X-ray source operating at 15 kV and 20 mA. The spectra were collected with analyser pass energy 20 eV, step 0.1 eV and an electron take off angle of 90° . The samples were pressed into thin wafers and degassed in a preparation chamber before analysis. The Shirley background subtraction and peak fitting with Gaussian–Lorentzian product peak was performed using a XPS processing program Advantage (Thermo Electron Corporation). The charging effects were corrected by adjusting the Ce $3d_{3/2}$ peak, usually described as u''' peak to a position of 917.00 eV [19–21]. This is a strong, individual peak and its position can be established much more precisely than that of the commonly used C 1s peak from adventitious carbon.

2.3. Catalytic activity measurements

The catalytic test of NO reduction by CO was performed using a quartz glass U-shaped reactor, equipped with a temperature programmed controller. The reactants and products were mon-

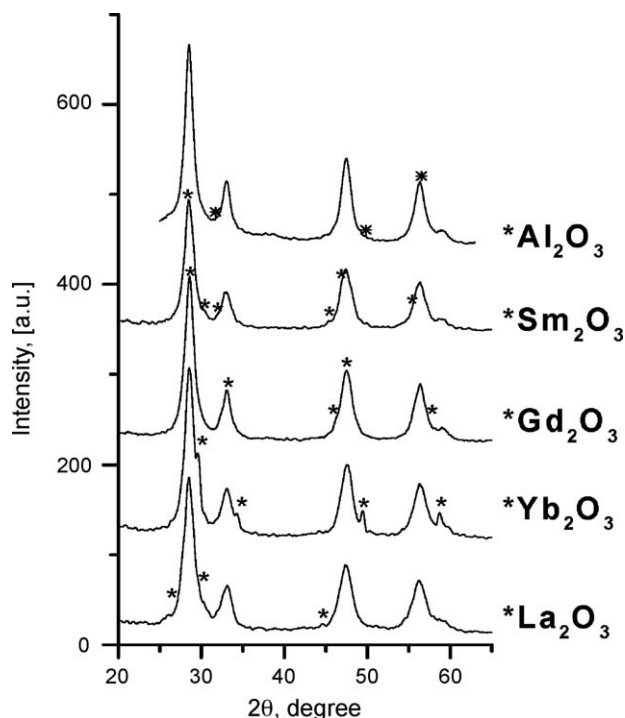


Fig. 1. XRD patterns of the studied gold catalysts: the lines of ceria and the corresponding oxides of the dopants (*).

itored by ABB IR and UV analysers. The QM (quadrupole mass) analysis of the reaction products was also performed using on-line Pfeiffer quadrupole mass spectrometer and Balzers Quadstar software. The conversion degree of NO and CO was taken as a measure of catalytic activity. The steady-state tests were made upon increasing the reaction temperature, waiting at each temperature for a constant conversion value. The catalysts were tested at temperatures up to 400 °C at a flow rate of 50 ml min⁻¹ corresponding to WHSV of 60 000 ml g⁻¹ h⁻¹. The sample's mass was 0.05 g. The pretreatment of the catalyst was provided according to the previously chosen conditions [11,12] using 5% H₂ in argon for 30 min at 120 °C. The catalytic activity tests were performed under two different conditions: (i) using a feed gas composition – 3000 ppm NO + 3000 ppm CO + 3000 ppm H₂ and (ii) in the presence of water – 1500 ppm NO + 3000 ppm CO + 1000 ppm H₂ + 5% H₂O. These conditions were chosen on

Table 1

BET surface areas, lattice parameters and average sizes of ceria particles.

Samples	S _{BET} (m ² g ⁻¹)	Ionic radii of Me ³⁺ dopants (Å)	Lattice parameter a of ceria ^a (Å)	Average size of ceria (nm)
AuCe	108	–	5.422	8.0
AuCeAl	105	Al ³⁺ – 0.535	5.419	9.6
AuCeLa	72	La ³⁺ – 1.160	5.427	8.0
AuCeSm	76	Sm ³⁺ – 1.079	5.424	8.5
AuCeGd	69	Gd ³⁺ – 1.053	5.422	8.8
AuCeYb	78	Yb ³⁺ – 0.985	5.415	8.8

^a The experimental error on the a parameter is estimated as ±0.005.

the basis of our previous investigation on NO reduction by CO [13]. The corresponding feed gas mixtures were prepared using pure argon as a diluent. The catalysts stability was tested keeping the sample at reaction conditions (ii) for 18 h at 200 °C and than 3 h at 400 °C.

3. Results

3.1. Catalysts characterization

The X-ray diffraction patterns, presented in Fig. 1, show the diffraction lines of CeO₂ typical of the cubic crystal structure of fluorite type oxide. For all lanthanide-containing catalysts two phases are present—in addition to ceria, the lines of the dopant oxides are also registered. The peaks of gold are not visible due to the low amount of loading and the small crystallites size. The average size of gold particles on the AuCeAl catalyst was 2.9 nm [13]. The average size of gold particles on the AuCe catalyst and gold catalysts on ceria doped by the lanthanides was lower than the XRD limit to about 3 nm and it was estimated by HRTEM. The data obtained were: 2.0 nm for AuCe [15,22], 2.4 nm for AuCeSm and 2.3 nm for AuCeLa [23]. The BET surface area, lattice parameters and the average particle size of ceria, determined by XRD are presented in Table 1. The data on AuCe are given for comparison as well. It is seen that the BET surface area of ceria doped by aluminum is higher compared to the case of ceria doped by lanthanides. The ceria supports are nano-structured having average particle sizes <10 nm. The values of lattice parameter a for the AuCeAl catalysts as well as Au catalysts supported on doped by La, Sm, Gd and Yb ceria are close to that of the AuCe one.

Fig. 2(A) and (B) shows the Raman spectra of the studied gold samples as well as those of the initial supports. The main line of CeO₂ dominates in the Raman spectra. In the case of CeSm and

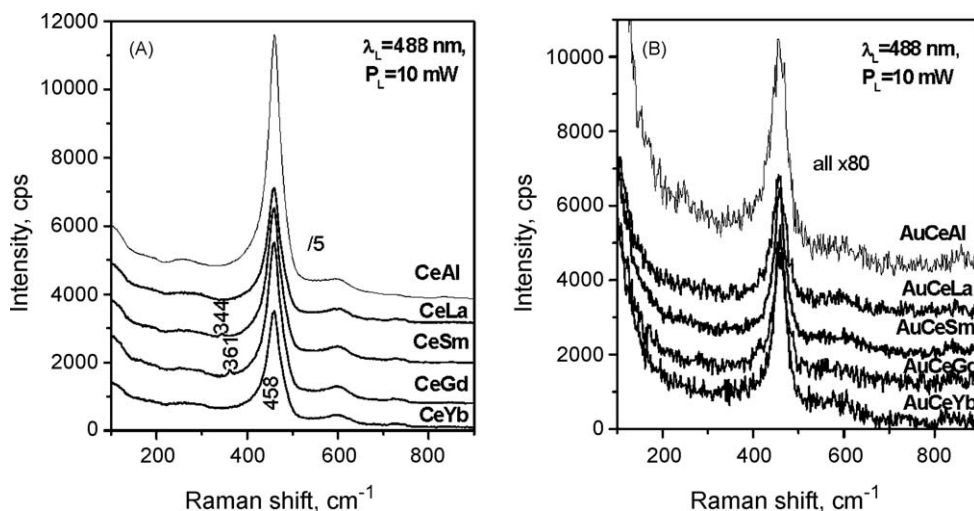


Fig. 2. Raman spectra of the initial supports (A) and the gold-containing catalysts (B).

Table 2

The position and the values of FWHM of the dominant ceria line in the Raman spectra of the initial supports and the gold catalysts.

Supports/ Au-catalysts	Supports		Gold catalysts	
	Position (cm^{-1})	FWHM (cm^{-1})	Position (cm^{-1})	FWHM (cm^{-1})
Ce/AuCe	464	12.0	462	13.5
CeAl/AuCeAl	459	34.0	456	39.4
CeLa/AuCeLa	458	37.4	457	36.6
CeSm/AuCeSm	458	36.8	458	29.7
CeGd/AuCeGd	458	36.4	458	30.0
CeYb/AuCeYb	458	36.8	459	32.2

CeGd, the typical lines of Sm_2O_3 (344 cm^{-1}) and Gd_2O_3 (361 cm^{-1}) are also registered. The loading of gold makes the spectra strongly absorbing. The position of the characteristic line of ceria for the Au-free supports and the corresponding gold catalysts, including undoped ceria (Ce) and gold supported on ceria (AuCe) are represented in Table 2. Compared to the undoped ceria, a shift to lower frequencies in the presence of all dopants is seen. Such shift has been observed by McBride et al. in their study on ceria doped by La, Pr, Nd, Eu, Gd and Tb [24]. The calculated values of the full width at the half of maximum (FWHM) of the ceria main line are compared in Table 2 and it will be discussed below.

Fig. 3 shows the TPR profiles of the fresh gold catalysts (A) and the TPR profiles after the reoxidation at 200°C (B). The presence of nanosized gold leads to a significant lowering of the temperatures for the reduction of ceria surface layers while the bulk reduction is not influenced [15,25]. In Fig. 3 only low-temperature (LT) TPR peaks associated with the reduction of surface layers of ceria are presented. Our previous studies of gold deposited on hardly reducible titania and zirconia supports [26,27] have shown that a reduction process of oxidized gold species also occurs at these temperatures but in the present case (2–2.9 wt.% of Au on a reducible support) the hydrogen consumption (HC) by the oxidized gold is negligible compared to that needed for the surface reduction of ceria. Concerning the TPR of fresh AuCeSm and AuCeLa samples, two overlapping peaks are

Table 3

Hydrogen consumption (HC) and degree of reduction from the TPR of fresh catalysts and after reoxidation.

Samples	TPR of fresh samples		TPR after reoxidation	
	HC ($\mu\text{mol g}^{-1}$)	Degree of reduction (%)	HC ($\mu\text{mol g}^{-1}$)	Degree of reduction (%)
AuCe	461	16.9	304	10.5
AuCeAl	352	13.5	322	12.3
AuCeLa	620	23.7	502	19.2
AuCeSm	718	27.5	558	21.3
AuCeGd	586	22.4	492	18.8
AuCeYb	598	22.9	488	18.7

recorded at $T_{\text{max}} = 117$ and 155°C , and $T_{\text{max}} = 109$ and 140°C , respectively. For AuCeGd sample the detected TPR peak is also complex with T_{max} at 118°C and a shoulder at 149°C . These results could suggest that the structure of ceria surface is not homogeneous, leading to the observation of two different TPR peaks. For the AuCeYb sample a single, symmetric and narrow TPR peak at $T_{\text{max}} = 125^\circ\text{C}$ was recorded, showing a homogeneous ceria surface. One single, but broader TPR peak with T_{max} at 125°C is observed also in the case of Al-containing gold catalyst. In all cases, after the reoxidation, the registered TPR peaks are broad and not very different in shape. The lowest T_{max} was observed for AuCeYb (78°C) and AuCeAl (80°C) catalysts. Table 3 gives also the data on HC and the corresponding degree of reduction for each catalyst, including the AuCe sample. Concerning the fresh catalysts, the lowest HC (lower than that of gold on undoped ceria) was observed for the AuCeAl sample. The results of TPR after reoxidation showed that the oxygen capacity was not fully recovered during the reoxidation and it remained lower than that of the fresh samples. Again the lowest HC among the catalysts based on modified ceria was observed for the AuCeAl sample. There are only small differences between the values of HC for the lanthanide-containing samples, the HC being higher for the AuCeSm catalyst.

The catalysts were characterized by means of XPS as well. The Au 4f XPS spectra of the fresh and spent samples (after experimental

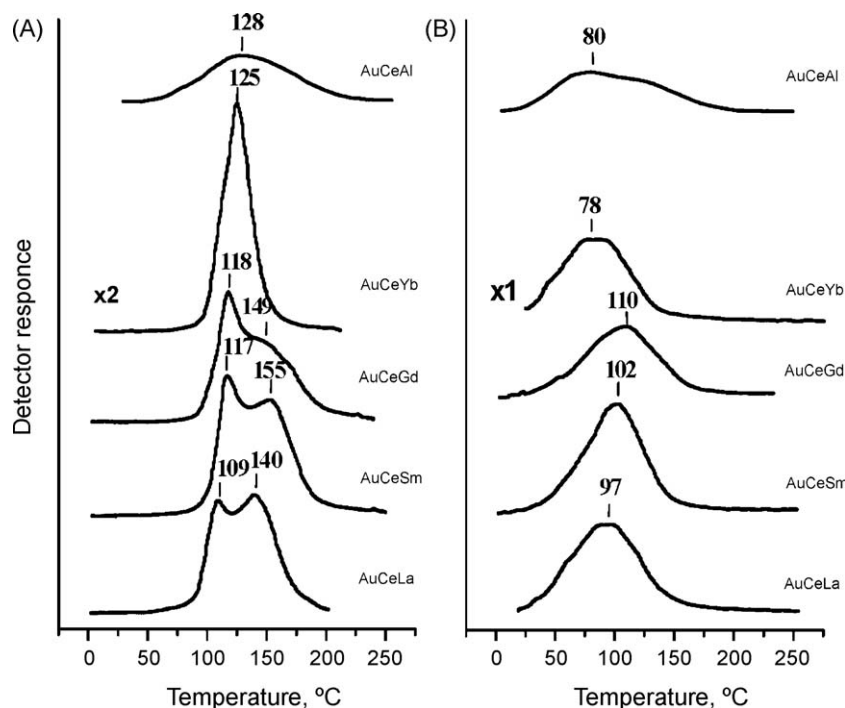


Fig. 3. TPR profiles of the fresh samples (A) and after reoxidation (B).

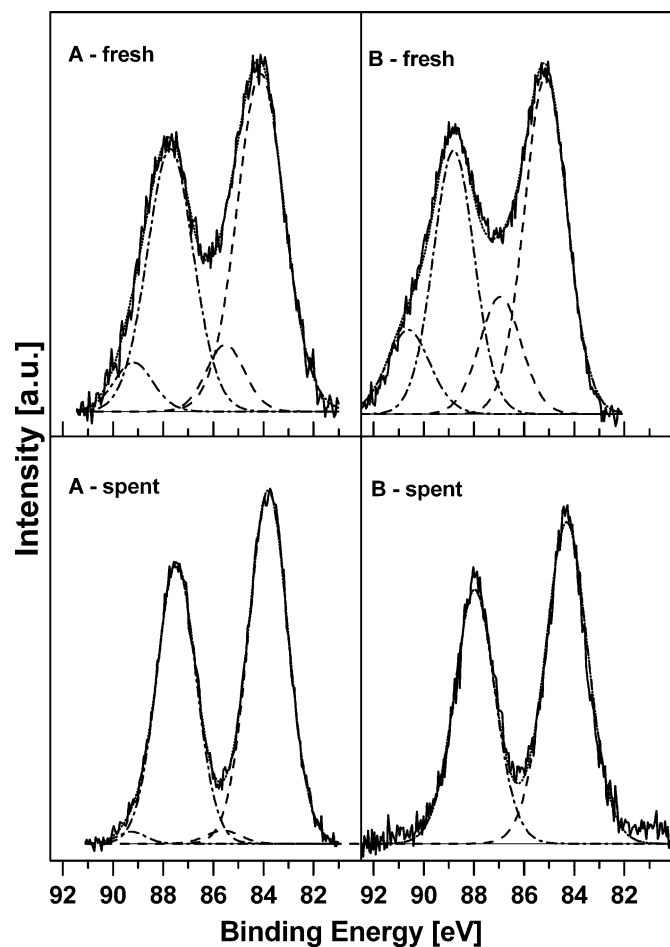


Fig. 4. Experimental and fitted Au 4f XPS spectra of Al and Yb-containing gold catalysts: fresh and after catalytic test following the experimental route (ii).

Table 4

Au 4f_{7/2} and Ce 3d_{5/2} BEs, along with the component percentages for gold catalysts: fresh and after the catalytic operation following route (ii).

Catalysts	Au 4f _{7/2}		Ce 3d _{5/2}	
	Peak position, BE (eV)	(%)	Peak position, BE (eV)	Ce ³⁺ (%)
AuCeAl-fresh	84.14 85.59	77.20 22.80	884.99 880.23	19.20
AuCeAl-spent	83.80 85.60	96.80 3.20	885.78 880.34	21.60
AuCeLa-fresh	84.13 85.28 86.35	20.15 59.70 20.15	884.91 881.11	26.90
AuCeLa-spent	84.49	100.00	885.40 880.17	18.30
AuCeSm-fresh	84.25 85.91	42.69 57.31	885.85 880.08	17.60
AuCeSm-spent	84.45	100.00	885.43 880.83	15.30
AuCeGd-fresh	85.29 87.23	80.53 19.47	884.94 880.84	18.80
AuCeGd-spent	84.29	100.00	885.59 879.69	15.10
AuCeYb-fresh	85.14 86.95	74.64 25.36	885.03 880.35	27.70
AuCeYb-spent	84.26	100.00	885.34 880.03	19.50

route (ii), containing Al and Yb as dopants, are presented in Fig. 4. The Ce 3d XPS spectra for the same samples are illustrated in Fig. 5. The XPS data of all samples studied are summarized in Table 4. The Au 4f XPS spectra of the fresh samples were fitted successfully with two or three Au components. According to the literature, the Au 4f_{7/2}

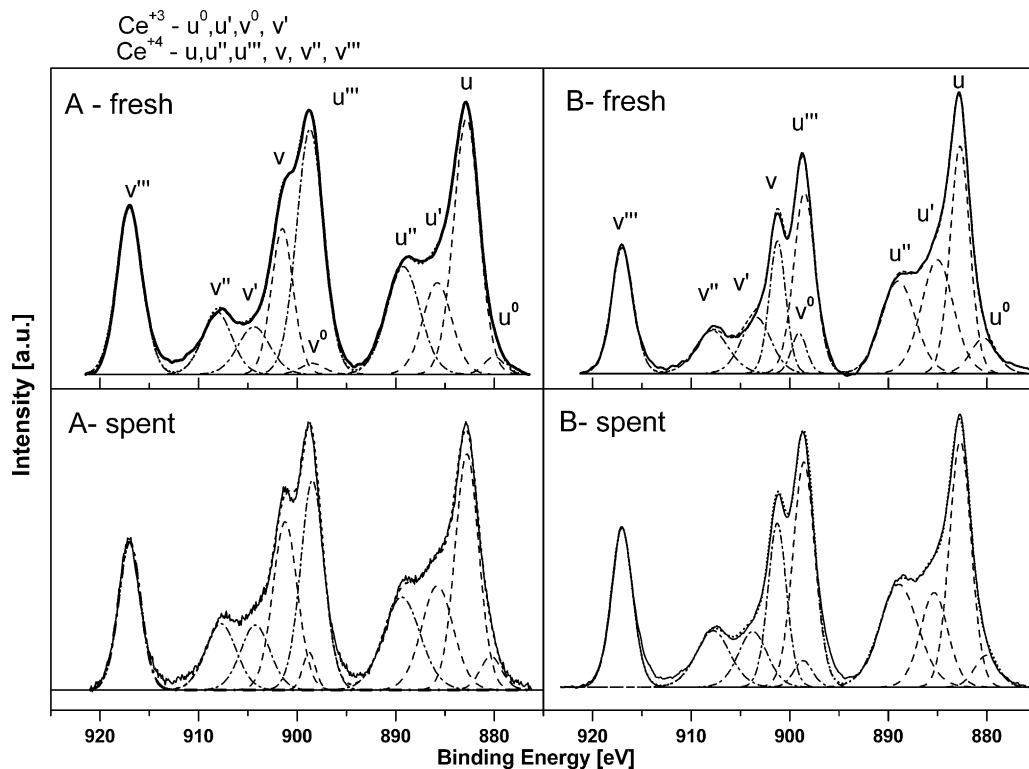


Fig. 5. Experimental and fitted Ce 3d XPS spectra of Al and Yb-containing gold catalysts: fresh and after catalytic test following the experimental route (ii).

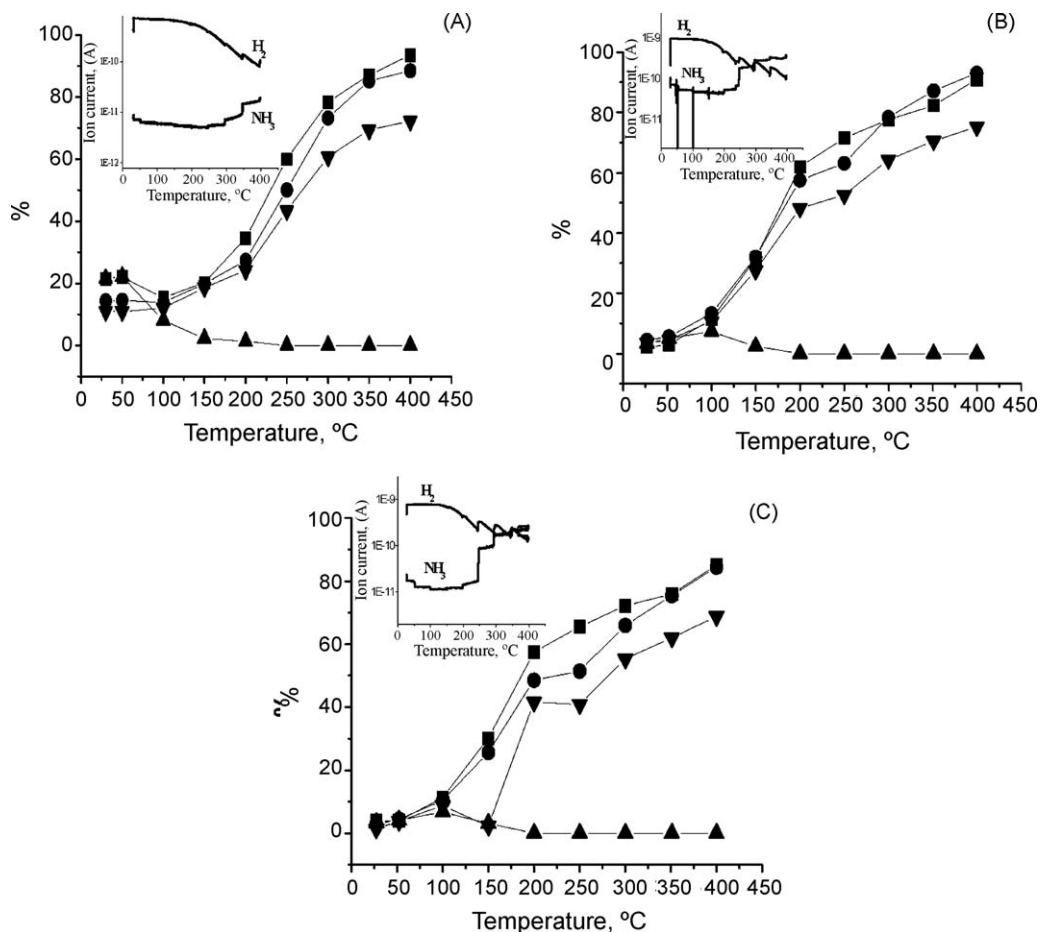


Fig. 6. Catalytic activity in the NO reduction by CO using 3000 ppm NO + 3000 ppm CO + 3000 ppm H₂ over AuCeAl (A), AuCeSm (B) and AuCeLa (C): (■) conversion of NO, (●) conversion of CO, (▲) formation of N₂O, (▼) formation of CO₂; in the inset the corresponding QM signals of H₂ and NH₃ are shown.

positioned at binding energy (BE) at 83.8/84.5 eV is assigned to the presence of metallic gold. The peaks located at BE shifted to higher values (85.1/85.6 eV) are related to positively charged gold particles or oxidized species (Au^{δ+} or Au¹⁺). The highest values of BE at 86.3/87.3 are assigned as ionic Au³⁺ [28,29]. Comparing all fresh samples of the catalysts doped by lanthanides and aluminum one can see that the relative contribution of the positively charged Au components is much higher for the catalysts doped by lanthanides than for the catalysts doped by aluminum. After catalytic processing the samples containing lanthanides exhibit only metallic gold on the surface whereas on the AuCeAl sample a small amount of positively charged gold particles was detected in addition to the metallic gold. Careful analysis of the Ce 3d XPS spectra allows distinguishing and quantifying the surface concentration of the Ce³⁺ and Ce⁴⁺ compounds. The estimated relative surface contribution of Ce³⁺ is presented in Table 4 (see Ce³⁺% column). Comparing the fresh and spent samples, a tendency of lowering the Ce³⁺ concentration is observed for samples containing lanthanides, while a slightly higher Ce³⁺ amount was found in the samples doped by aluminum.

3.2. Catalytic activity measurements

The catalytic activity results of the studied gold catalysts on doped ceria differ, depending on the chosen experimental conditions. Fig. 6 represents the results on AuCeAl (A), AuCeSm (B) and AuCeLa (C) catalysts, using a feed gas composition: 3000 ppm NO + 3000 ppm CO + 3000 ppm H₂. The data obtained by quadrupole mass spectrometer (QM) are shown in the inset. It is

seen that in all cases a small amount of N₂O was formed only at temperatures up to 150 °C, the NH₃ formation started at about 220–230 °C for AuCeAl and at 250 °C for AuCeSm and AuCeLa catalysts. The selectivity toward N₂ was 100% at about 200 °C and at this temperature the higher NO and CO conversion (61.9% and 57.5%, respectively) was observed with the AuCeSm sample, the lowest values (35% and 25%, respectively) were obtained for the AuCeAl one. During the catalytic test using a feed gas composition: 1500 ppm NO + 3000 ppm CO + 1000 ppm H₂ + 5% H₂O, a significant improvement of both NO and CO reduction was achieved over all studied catalysts (Fig. 7). At 200 °C the highest conversion of NO (85%) and CO (89%) was established for the AuCeYb catalyst. At 250 °C both NO and CO conversions were above 90% for all of the studied catalysts. Again in all cases some amount of N₂O was registered below 150 °C. However, the QM monitoring (Fig. 7, inset) showed substantial differences in the NH₃ formation when comparing the gold catalyst supported on ceria doped by aluminium and ceria doped by lanthanides. Like in the case without water in the feed, NH₃ formation started above 220 °C over the AuCeAl catalyst, while for all gold catalysts containing lanthanides no NH₃ was registered up to 400 °C.

The test of stability, performed on the AuCeYb catalyst (the catalyst which exhibited the highest activity) after second experimental route (conditions, described in Section 2) showed that the loss of activity at the end of the 15 h of testing at 200 °C was 13% and no more changes in the NO and CO conversions were established during the next 3 h at the same temperature. During the subsequent 3 h catalytic operation at 400 °C the NO and CO conversions achieved stable values of 100%.

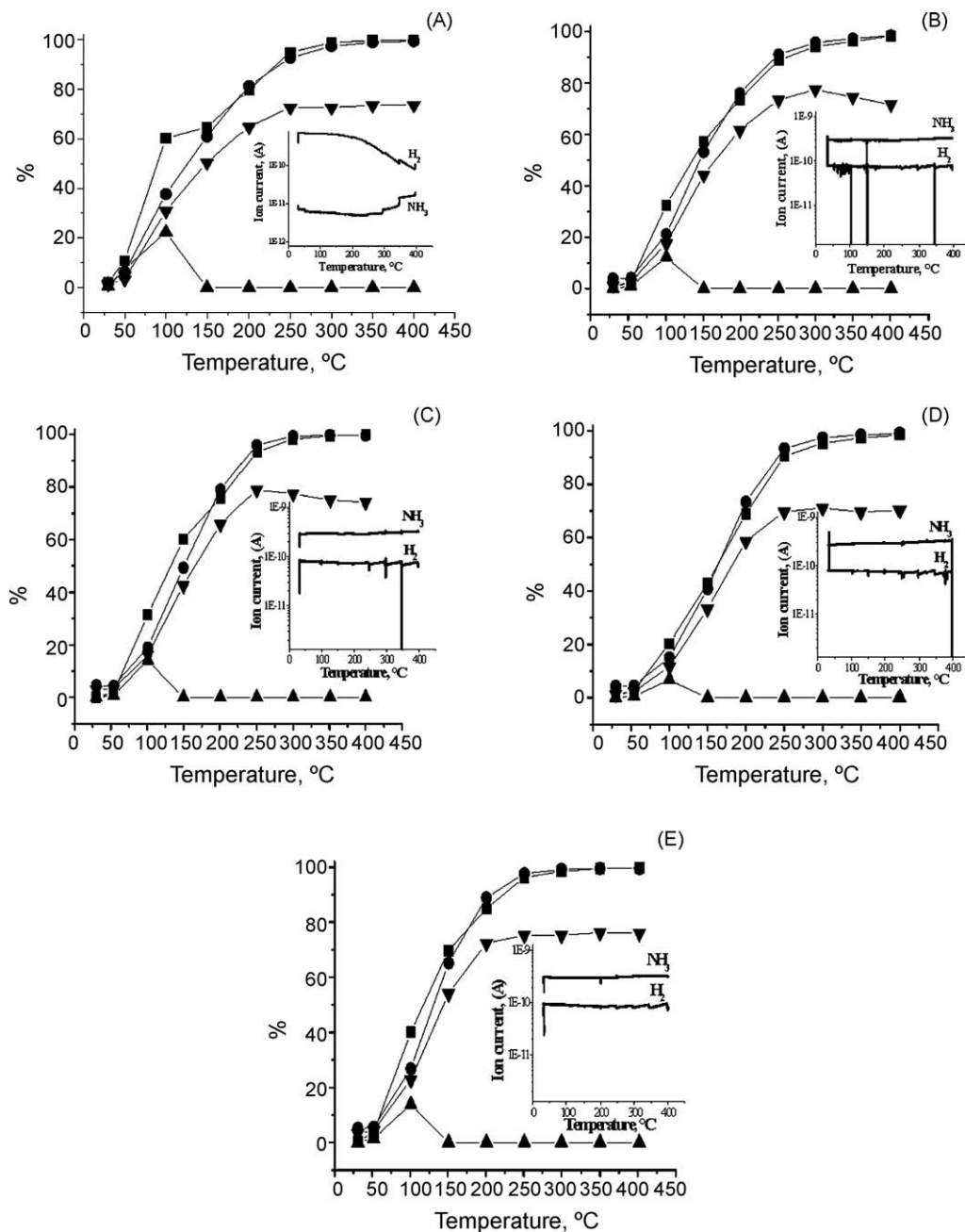


Fig. 7. Catalytic activity in the NO reduction by CO using 1500 ppm NO + 3000 ppm CO + 1000 ppm H₂ + 5% H₂O over AuCeAl (A), AuCeSm (B); AuCeLa (C), AuCeGd (D) and AuCeYb (E): (■) conversion of NO, (●) conversion of CO, (▲) formation of N₂O, (▼) formation of CO₂; in the inset the corresponding QM signals of H₂ and NH₃ are shown.

4. Discussion

The loading of gold on ceria causes a strong modification, resulting in the creation of oxygen vacancies and Ce³⁺ [22,30]. As the ionic radius of Ce³⁺ (1.14 Å) is larger than that of Ce⁴⁺ (0.97 Å), the generated Ce³⁺ ions cause an increase of the lattice parameter *a* of ceria from 5.412 Å (undoped ceria) to 5.422 Å (AuCe sample). Due to the applied MA preparation method, the values of lattice parameter *a* for the Au catalysts supported on doped ceria are not very different than that of the AuCe sample. There are no substantial differences in the average sizes of gold and ceria nano-particles of the catalysts.

It is an open question how the lanthanides and aluminum dopants affect the chemical nature of gold loaded on ceria support. As noted above both zero-valent gold and positively charged gold species, can be formed during the catalysts

preparation. The oxidized form of gold originates most likely from very small Au crystallites strongly interacting with the ceria support, which are able to coordinate more oxygen species due to their high surface unsaturation. The XPS allows to distinguish and quantify the surface concentration of all coexisting Au species. The analysis of the XPS data presented in Table 4 indicates that the contribution of the Au³⁺ species in the samples doped by lanthanides is significantly higher than that in the sample doped by Al. This is in accordance with the higher average size of gold in the AuCeAl sample since the positive charge is related to the existence of very small gold particles or to the periphery of gold particles, having high unsaturation (the periphery is higher for smaller particles). The obtained results suggest that the amount of the gold particles with a very small dimension can be affected also by the chemical nature of the other dopants loaded on ceria support.

The nature of the modifier and the method of its incorporation into ceria determine most likely the differences observed in the Raman and TPR data, as well as the catalytic activity results. It is known, that the broadening of the main line of ceria in the Raman spectra depends on ceria dispersion as well as on the defective structure of ceria, particularly on the amount of generated oxygen vacancies [31,32]. Having in mind the small differences in the average particles size of ceria (Table 1), the observed significant broadening of the FWHM for doped ceria in comparison with undoped ceria (Table 2), should be due to the formation of oxygen vacancies after introducing the modifiers. Very small differences are observed between the FWHM values of the initial supports doped by lanthanides. In the case of CeAl the broadening is lower, e.g. a lower amount of oxygen vacancies is caused by Al³⁺. This is in accordance with the mechanisms for crystal lattice compensation proposed by Trovarelli [14]. The addition of gold to the samples containing lanthanides causes decrease in the FWHM values. The gold catalyst supported on ceria doped by aluminum seems to be with the most defective ceria structure. This result is not in agreement with the TPR data because the lowest HC was observed for the AuCeAl catalyst (see Table 3). Our previous results on gold supported on ceria–alumina prepared by different methods and with different alumina content [11,13], have shown higher HC for the samples with higher values of FWHM, e.g. larger amount of oxygen vacancies. These results are reasonable as the presence of oxygen vacancies in the ceria structure enhances the oxygen mobility and consequently, the reduction process is also enhanced.

The HCs of gold catalysts supported on ceria doped by the lanthanides are significantly higher in comparison to that of AuCe, the highest HC being that of the AuCeSm. According to the literature data, the reduction of ceria surface layers is limited to 17% [33] or 20% [34]. Values higher than 20% of reduction degrees were obtained for the gold catalysts on ceria modified by the lanthanides. The reduction processes should be enhanced by the presence of dopants and could be related to some sub-surface layers of ceria. Within such a low temperature interval, the mobility of oxygen from the deeper layers is not very likely. It has to be taken also into account that a small amount of hydrogen could be retained into the bulk of ceria as well [34,35].

The catalytic activity results in the case of adding only hydrogen to the feed gas (experimental route (i)) correlates with the observed HCs (Table 3)—the lowest activity is exhibited by the AuCeAl catalyst (Fig. 6). For this sample the HC was the lowest in both direct TPR and TPR after reoxidation. Such correlation with TPR results has been already observed in the investigation of the NO reduction by CO over gold catalysts on CeO₂–Al₂O₃ supports with different alumina amount, prepared by CP or MA techniques [11,13]. The observed HCs were systematically higher for the CP samples, which exhibited higher catalytic activity in the CO + NO reaction (hydrogen was also present in the feed) compared to the MA ones. Regarding both preparation methods, higher activities were observed and larger values of HC were calculated for gold catalysts with higher alumina content. It has been assumed that the higher catalytic activities are associated with the higher amount of oxygen vacancies and defects in the ceria structure. When using the CP method for synthesis of the mixed supports and higher alumina content, more defective ceria structure has been obtained. It caused larger FWHM value of the main line of ceria in the Raman spectra. In the present study, the AuCeAl catalyst exhibited the lowest activity in the NO reduction by CO (experimental route (i), Fig. 6) as well as the lowest HC obtained by both direct TPR and TPR after reoxidation. At the same time, as mentioned above, the FWHM value of the AuCeAl catalyst was higher than those of the gold catalysts supported on ceria modified by the lanthanides (Table 2). At the moment we do not have an exact explanation of this experimental fact. The possible explana-

tion could be that the amount of oxygen vacancies in ceria formed in the presence of lanthanides exceeds that caused by Al (as it has been found for the Au-free supports in agreement with Trovarelli [14]). However, the decrease in FWHM values obtained after the deposition of gold could suggest that during the preparation of the gold catalysts, the oxygen vacancies were driven in the vicinity of the lanthanide ions, making the ceria structure not so defective according to the Raman spectroscopy data.

Under all experimental conditions employed, the formation of N₂O was observed only up to 150 °C. We reported earlier [11,12] that the addition of increasing amounts of H₂ boosted the catalytic activities of similar gold catalysts supported on co-precipitated (CP) ceria–alumina in the reduction of NO by CO. However, according to the results of previous study [13] on the NO reduction with hydrogen (without CO in the gas feed), the reduction activity of H₂ was very low in the LT range. High conversion of NO to ammonia started above 250 °C. Although the hydrogen is not very effective reducing agent within the LT interval, it assists the NO reduction by CO. Recent *in situ* FTIR investigations have shown that the role of H₂ is to keep the ceria surface reduced, creating oxygen vacancies as active sites for the dissociation of NO [36]. This can explain the observed relationship between the catalytic activity and reducibility of the gold catalysts studied. At higher temperatures, the H₂ uptake is due also to the formation of NH₃.

Interesting results were obtained, following the experimental route (ii) with water-containing feed gas (Fig. 7). On the one hand, based on the results of previous investigations [13], a significant improvement of the catalytic activity of all gold catalysts in the presence of water should be expected. The effect of water can be related to the additional amount of hydrogen produced via WGS reaction.

All gold catalysts in the present study exhibit high degree of NO and CO conversion when water was added to the feed gas. The observed high activity is in agreement with the high amount of oxygen vacancies deduced from the TPR and Raman spectroscopy results and correlates well with the high surface concentration of the Ce³⁺ species on the spent samples (experimental route (ii)) estimated by XPS data. The catalytic activity of gold catalyst supported on ceria doped by Yb is somewhat higher. This correlates with the observed redox activity. For the fresh AuCeYb sample a single narrow TPR peak was recorded, showing a higher surface homogeneity compared to the other lanthanides (two overlapping TPR peaks). For the same catalyst, the lowest $T_{\max} = 78$ °C was recorded after the reoxidation. Upon adding water to the feed, the NO and CO degrees of conversion for the AuCeAl catalyst were relatively close to that of the AuCeYb one. The direct TPR of the AuCeYb catalyst did not show also a double TPR peak as in the case of Sm, La and Gd. The TPR peak after the reoxidation of AuCeAl is at $T_{\max} = 80$ °C. It should be noted that the AuCeYb catalyst showed the highest activity in the WGS reaction among the gold catalysts supported on ceria doped by the other lanthanides [23]. Regarding the catalysts based on ceria–alumina (CP or MA with different alumina content), the AuCeAlMA (10 wt.% alumina) exhibited the highest WGS activity [22]. A relationship between the catalytic activity in the NO + CO reaction in the presence of water and catalytic activity in the WGS reaction has to be taken into consideration.

On the other hand, very promising results related to the selectivity toward N₂ were achieved for gold catalysts supported on ceria doped by lanthanides. In contrast to the results on the AuCeAl sample, no NH₃ was registered within the whole temperature interval up to 400 °C under moist feed. The reason for this could be that the ammonia formation did not occur or that the rate of NO reduction by NH₃ is very high.

The results of QM monitoring (Fig. 7, the inset) showed that there is no uptake of H₂ over the gold catalysts doped by La, Sm, Gd

and Yb. The most probable reason for this seems to be that in the presence of lanthanides ammonia was not formed by the reduction of NO with H₂ and that the amount of H₂ needed to keep the surface reduced is compensated by that produced in the WGS reaction. The results with moist feed gas show that using the lanthanides as modifiers, the accidental overheating in the catalytic bed should not lead to a decrease of the selectivity as in the case of ceria doped by aluminum.

5. Conclusions

The modification of ceria by Me³⁺ (Me = Al, La, Sm, Gd and Yb) using MA method of preparation causes a small change in the lattice parameter of CeO₂, depending on the ionic radius of the dopant. There is no substantial influence on the average size of gold and ceria nano-particles. The method applied for support preparation leads to the formation of some amount of lanthanide oxide phase in addition to the phase of modified ceria. The XPS data reveal that the concentration of the oxidized gold species is higher than the concentration of metallic Au in the fresh samples modified by the lanthanides. On the fresh samples modified by Al only a small part of metallic gold exists in oxidized state. After the catalytic test, only metallic gold was found on the lanthanide-containing catalysts while on the Al₂O₃-modified catalyst a small amount of oxidized Au species in addition to metallic Au has been detected. Higher FWHM values of the main ceria line in the Raman spectra of the Au-free supports doped by lanthanides were found, while in the case of ceria–alumina the broadening of the same line was smaller. The addition of gold resulted in different FWHM values depending on the nature of the modifier. Among the gold catalysts, the ceria structure seems to be the most defective in the presence of aluminum as a dopant. This result does not agree with the TPR data. For the alumina-containing catalyst the observed lowest HC in the direct TPR as well as in the TPR after reoxidation, correlates with the lowest activity in the NO reduction by CO, when hydrogen is present in the feed gas. The addition of water to the feed causes significant improvement of the NO and CO conversions over all of the samples studied. The high surface concentration of the Ce³⁺ species on the spent samples, revealed from the XPS data analysis, correlates well with the high catalytic activity. Yb-containing gold catalyst exhibited the highest NO and CO conversion (85% and 89%, respectively) at 200 °C. Very promising results for the selectivity toward N₂ were achieved using the lanthanides as dopants. In contrast to the results on gold supported on aluminum-doped ceria, no NH₃ formation was observed within the whole temperature interval up to 400 °C over gold catalysts supported on ceria modified by the lanthanides.

Acknowledgments

This research study has been performed in the framework of a D36/003/06 COST program and a NATO grant CBP.EAP.

CLG982799. L.I., I.I., R.N. and D.A. gratefully acknowledge the support by National Science Fund, Ministry of Education and Sciences of Bulgaria (project X-1502). The authors thank to Prof. K. Petrov for the assistance and helpful comments concerning the XRD results.

References

- [1] M. Haruta, N. Yamada, T. Kobayashi, S. Iijima, *J. Catal.* 115 (1989) 301.
- [2] S. Sakurai, S. Tsubota, M. Haruta, *Appl. Catal. A: Gen.* 102 (1993) 125.
- [3] G. Bond, C. Louis, D. Thompson, in: G. Hutchings (Ed.), *Catalysis by Gold*, Catal. Sci. Series, vol. 6, Imperial College Press, London, 2006.
- [4] T.M. Salama, R. Ohnishi, T. Shido, M. Ichikawa, *J. Catal.* 162 (1996) 169.
- [5] A. Ueda, M. Haruta, *Gold Bull.* 32 (3) (1999) (and references therein).
- [6] M.C. Kung, J.-H. Lee, H.H. Kung, *Am. Chem. Soc., Div. Fuel Chem.* 40 (1995) 1073.
- [7] M.A.P. Dekkers, M.J. Lippits, B.E. Nieuwenhuys, *Catal. Today* 54 (1999) 381.
- [8] J.R. Mellor, A.N. Palazov, B.S. Grigorova, J.F. Greyling, K. Reddy, M.P. Letsoalo, J.H. Marsh, *Catal. Today* 72 (2002) 145.
- [9] E. Seker, E. Gulari, *Appl. Catal. A: Gen.* 232 (2002) 203.
- [10] A.C. Gluhoi, S.D. Lin, B.E. Nieuwenhuys, *Catal. Today* 90 (2004) 175.
- [11] L. Ilieva, G. Pantaleo, I. Ivanov, A.M. Venezia, D. Andreeva, *Appl. Catal. B: Environ.* 65 (2006) 101.
- [12] L. Ilieva-Gencheva, G. Pantaleo, N. Mintcheva, I. Ivanov, A.M. Venezia, D. Andreeva, *J. Nanosci. Nanotechnol.* 8 (2008) 867.
- [13] L. Ilieva, G. Pantaleo, J.W. Sobczak, I. Ivanov, A.M. Venezia, D. Andreeva, *Appl. Catal. B: Environ.* 76 (2007) 107.
- [14] A. Trovarelli, *Catal. Rev. -Sci. Eng.* 38 (1996) 439.
- [15] D. Andreeva, V. Idakiev, T. Tabakova, L. Ilieva, P. Falaras, A. Bourlinos, A. Travlos, *Catal. Today* 72 (2002) 51.
- [16] W. Kraus, G. Nolze, *PowderCell for Windows*, Version 2.4, Federal Institute for Materials Research and Testing, Rudower Chaussee, Berlin, Germany.
- [17] N. Kotzev, D. Shopov, *J. Catal.* 22 (1971) 297.
- [18] D.A.M. Monti, A. Baiker, *J. Catal.* 83 (1983) 323.
- [19] M. Romeo, K. Bak, J. El Fallah, F. Le Normand, *Surf. Interf. Anal.* 20 (1993) 508.
- [20] L. Armelao, D. Barecca, G. Bottaro, A. Gasparotto, E. Tondello, *Surf. Sci. Spectra* 8 (2001) 247.
- [21] A.Q. Wang, P. Panchaipetch, R.M. Wallace, T.D. Golden, *J. Vac. Sci. Technol. B* 21 (2003) 1169.
- [22] D. Andreeva, I. Ivanov, L. Ilieva, J.W. Sobczak, G. Avdeev, K. Petrov, *Topics Catal.* 44 (2007) 173.
- [23] D. Andreeva, I. Ivanov, L. Ilieva, M.V. Abrashev, R. Zanella, J.W. Sobczak, W. Lisowski, M. Kantcheva, G. Avdeev, K. Petrov, *Appl. Catal. A: Gen.* 357 (2009) 159.
- [24] J.R. McBride, K.C. Hass, B.D. Poindexter, W.H. Weber, *J. Appl. Phys.* 76 (1994) 2435.
- [25] Q. Fu, A. Weber, M. Flytzani-Stephanopoulos, *Catal. Lett.* 77 (2001) 87.
- [26] D. Andreeva, T. Tabakova, L. Ilieva, A. Naydenov, D. Mehanjiev, M.V. Abrashev, *Appl. Catal. A: Gen.* 209 (2001) 291.
- [27] L. Ilieva, J.W. Sobczak, M. Manzoli, B.L. Su, D. Andreeva, *Appl. Catal. A: Gen.* 291 (2005) 85.
- [28] M.P. Casaletto, A. Longo, A. Martorana, A. Prestianni, A.M. Venezia, *Surf. Interf. Anal.* 38 (2006) 215.
- [29] G.J. Hutchings, M.S. Hall, A.F. Carley, P. Landon, B.E. Solsona, C.J. Kiely, A. Herzing, M. Makkee, J.A. Moulijn, A. Overweg, J.C. Fierro-Gonzalez, J. Guzman, B.C. Gates, *J. Catal.* 242 (2006) 71.
- [30] T. Tabakova, F. Boccuzzi, M. Manzoli, D. Andreeva, *Appl. Catal. A: Gen.* 252 (2003) 385.
- [31] G.W. Graham, W.H. Weber, C.R. Peters, R. Usmen, *J. Catal.* 130 (1991) 310.
- [32] I. Kosacki, T. Suzuki, H.U. Anderson, Ph. Colomban, *Solid State Ionics* 149 (2002) 99.
- [33] M.G. Sanchez, J.L. Gazquez, *J. Catal.* 104 (1987) 120.
- [34] A. Laachir, V. Perrichon, A. Bardi, J. Lamotte, E. Catherine, J.C. Lavalley, J. El Faallah, L. Hilaire, F. le Normand, E. Quemere, G.N. Sauvion, O. Touret, *J. Chem. Soc. Faraday Trans.* 87 (1991) 1601.
- [35] J.L.G. Fierro, J. Soria, J. Sanz, J.M. Rojo, *J. Solid State Chem.* 66 (1987) 154.
- [36] M. Kantcheva, O. Samarskaya, L. Ilieva, G. Pantaleo, A.M. Venezia, D. Andreeva, *Appl. Catal. B: Environ.* (2008), doi:10.1016/j.apcatb.2008.09.023.